HHS Public Access

Author manuscript

Cell Rep. Author manuscript; available in PMC 2019 June 17.

Published in final edited form as:

Cell Rep. 2018 April 17; 23(3): 808–822. doi:10.1016/j.celrep.2018.03.092.

Platelets Promote Metastasis via Binding Tumor CD97 Leading to Bidirectional Signaling that Coordinates Transendothelial Migration

Yvona Ward[1,7], **Ross Lake**[1,7], **Farhoud Faraji**[2], **Jamie Sperger**[3], **Philip Martin**[4], **Cameron Gilliard**[5], **Kimberly P. Ku**[3], **Tamara Rodems**[3], **David Niles**[6], **Heather Tillman**[1], **JuanJuan Yin**[1], **Kent Hunter**[2], **Adam G. Sowalsky**[1], **Joshua Lang**[3], and **Kathleen Kelly**[1,8,*]

[1]Laboratory of Genitourinary Cancer Pathogenesis, NCI, Bethesda, MD 20892, USA

[2]Laboratory of Cancer Biology and Genetics, NCI, Bethesda, MD 20892, USA

[3]Carbone Cancer Center, University of Wisconsin-Madison, Madison, WI 53705, USA

[4]Center for Advanced Preclinical Research, NCI, Frederick, MD 21702, USA

[5]Molecular Biology and Genetics Section, NIDDK, Bethesda, MD 20892, USA

[6]Depatment of Biomedical Engineering, University of Wisconsin-Madison, Madison, WI 53705, USA

[7]These authors contributed equally

[8]Lead Contact

SUMMARY

Tumor cells initiate platelet activation leading to the secretion of bioactive molecules, which promote metastasis. Platelet receptors on tumors have not been well-characterized, resulting in a critical gap in knowledge concerning platelet-promoted metastasis. We identify a direct interaction between platelets and tumor CD97 that stimulates rapid bidirectional signaling. CD97, an adhesion G protein-coupled receptor (GPCR), is an overexpressed tumor antigen in several cancer types. Purified CD97 extra-cellular domain or tumor cell-associated CD97 stimulated platelet activation. CD97-initiated platelet activation led to granule secretion, including the release of ATP, a mediator of endothelial junction disruption. Lysophosphatidic acid (LPA) derived from platelets induced tumor invasiveness via proximal CD97-LPAR heterodimer signaling, coupling coincident tumor cell migration and vascular permeability to promote transendothelial migration. Consistent with this, CD97 was necessary for tumor cell-induced vascular permeability *in vivo* and metastasis

*Correspondence: kellyka@mail.nih.gov.

AUTHOR CONTRIBUTIONS

Y.W., R.L., F.F., J.S., J.L., and K.K. designed experiments. Y.W., R.L., F.F., J.J.Y., J.S., K.P.K., T.R., D.N., C.G., A.G.S., and J.L., performed experiments and/or analyzed data. H.T. and P.M. performed pathology analyses. K.H. provided reagents. Y.W. and K.K. wrote the manuscript. All authors provided critical comments on the manuscript.

SUPPLEMENTAL INFORMATION

Supplemental Information includes Supplemental Experimental Procedures and five figures and can be found with this article online at https://doi.org/10.1016/j.celrep.2018.03.092.

DECLARATION OF INTERESTS

J.L. holds equity in Salus, LLC which has licensed the VERSA technology used in these studies.

formation in preclinical models. These findings support targeted blockade of tumor CD97 as an approach to ameliorate metastatic spread.

Graphical Abstract

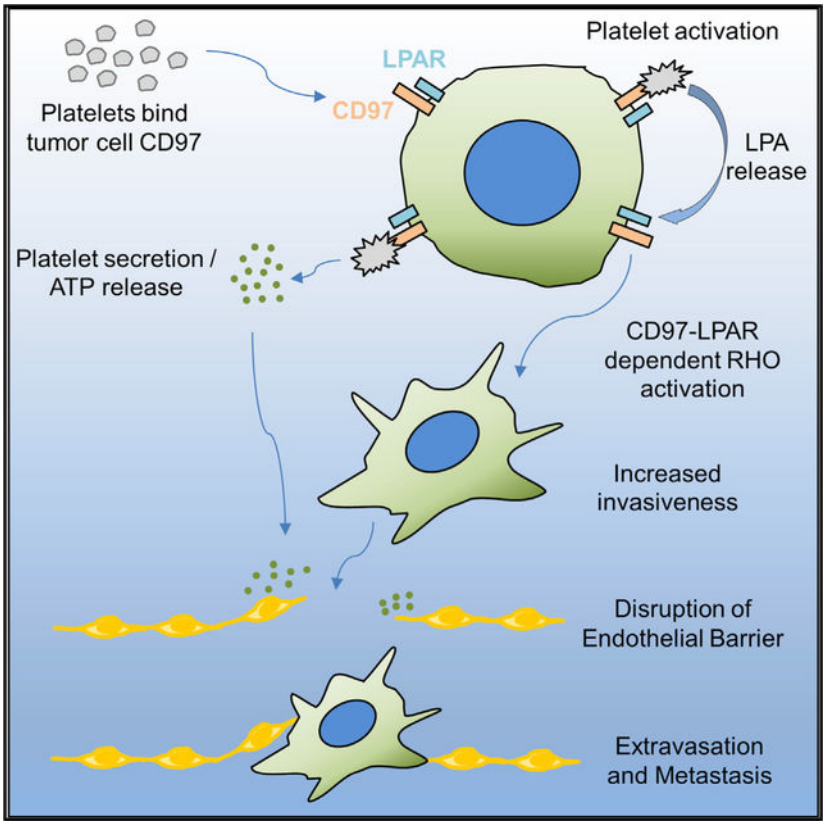

In Brief

Tumor-initiated platelet activation promotes tissue invasion of cancer cells and metastasis. Ward et al. demonstrate that a common tumor-associated antigen, CD97, accounts for platelet activation and participates directly in LPA-mediated signal transduction leading to tumor cell invasion. CD97 promotes vascular extravasation and metastasis in pre-clinical models.

INTRODUCTION

A critical goal of cancer research is limiting metastasis, the major cause of cancer patient mortality. The interaction of platelets and tumor cells has been shown experimentally to influence metastasis as a result of both physical association and bidirectional activation (Erpenbeck and Schön, 2010; Labelle and Hynes, 2012; Stegner et al., 2014). Platelet cloaking protects circulating tumor cells from sheer forces and from attack by the immune system (Nieswandt et al., 1999; Palumbo et al., 2005). Thrombi composed of tumor cells, platelets, and hematopoietic cells promote vascular adhesion and transendothelial migration (TEM) (Im et al., 2004; Schumacher et al., 2013). Platelet granule release plays a critical role in ATP-dependent endothelial retraction (Schumacher et al., 2013) and transforming

growth factor β (TGF-β) stimulated tumor cell motility and invasiveness (Labelle et al., 2011). The release of another soluble mediator, lysophosphatidic acid (LPA), is stimulated by platelet-tumor cell interactions (Boucharaba et al., 2004; Leblanc et al., 2014) and promotes experimental bone metastasis (Boucharaba et al., 2004). Metastasis is reduced in experimental models following genetic or pharmacologic inhibition of platelet activation and aggregation (Erpenbeck and Schön, 2010; Gasic et al., 1968; Labelle and Hynes, 2012). A critical step in platelet activation is the "inside-out" signaling that leads to a conformational switch activating integrin $\alpha_{IIb}\beta_3$, which enables ligation to various autocrine and paracrine factors that contribute to further activation and aggregation (Hynes, 2002; Shen et al., 2013). Several studies aimed at blocking integrin $\alpha_{IIb}\beta_3$ with inhibitors such as eptifibatide or abciximab have demonstrated inhibitory effects upon metastasis (Amirkhosravi et al., 2003; Boucharaba et al., 2004; Millard et al., 2011).

A central unanswered question, which could inform targeting tumor-platelet interactions, is the nature and context of cancer cell ligands capable of initiating platelet secretion and aggregation. Various properties of the adhesion G protein-coupled receptor (GPCR), CD97/ADGRE5, suggested it as a platelet receptor on tumor cells. Adhesion GPCRs are thought to mediate cell-cell and cell-matrix interactions and signaling (Langenhan et al., 2013). Adhesion GPCRs are bipartite structures processed from a single polypeptide to produce a large adhesive extracellular domain (termed the N-terminal fragment, NTF) and a noncovalently associated class B GPCR (termed the C-terminal fragment, CTF) (Araç et al., 2012). There are examples of both coordinated and independent functions for the extracellular (NTF) and GPCR (CTF) domains in this family of receptors (Langenhan et al., 2013; Petersen et al., 2015). The extracellular domain of CD97 contains between three and five epidermal growth factor (EGF)-like repeats and binds multiple ligands, including $\alpha_5\beta_1$ and $\alpha_v\beta_3$ integrins (Wang et al., 2005), CD55 (Hamann et al., 1996), CD90 (Wandel et al., 2012), and chondroitin sulfate (Stacey et al., 2003). These ligand interactions may exemplify a primarily adhesive function for CD97 because stimulation of GPCR signaling with the above referenced ligands has not been observed (Langenhan et al., 2013). On the other hand, CD97 forms a chimeric receptor with the LPA receptor (LPAR) GPCR, which leads to the amplification of LPA-stimulated Ga12/13 signaling (Ward et al., 2011, 2013). In normal tissues, CD97 expression is predominantly within hematopoietic cells (Jaspars et al., 2001), but abnormal CD97 expression as a tumor antigen occurs in a number of common epithelial malignancies (Safaee et al., 2013). Here, we provide evidence for a CD97-dependent mechanism that contributes to epithelial metastasis by promoting platelet activation and tumor cell signaling.

RESULTS

Platelet Activation Is Mediated by Adhesion to CD97

To investigate the effect of platelet interaction with human CD97 (hCD97), we used an adhesion assay whereby platelets were incubated with immobilized, purified CD97 protein fragments (Figure S1A). The full-length extracellular NTF domain up to the proteolytic processing site at amino acid (aa) 531 contains either 5 EGF (5E) or 3EGF (3E) repeats, an RGD sequence, and a mucin stalk fused to a mouse Fc region. CD97 5E and 3E fragments

stimulated platelets to flatten, protrude lamellipodia, and cluster, demonstrating morphological activation associated with granule secretion (Figures 1A and 1B) (Jin et al., 2009). Analyses of subfragments revealed that platelet morphological activation occurred upon contact with a fragment containing the 3 COOH-proximal EGF repeats and the adjacent region (aa 257–374) including the RGD tripeptide [E/3–5 RGD(374)] (Wang et al., 2005). By comparison, platelets bound but were not morphologically activated by fragments that included two EGF repeats and the adjacent region to aa 374 [E/4–5 RGD(374)] or by all five EGF repeats without the adjacent region (E/1–5) (Figures 1B and 1C). These data suggest that activation of platelets by recombinant CD97 was not mediated by a linear determinant, but instead, may involve more than one binding site or a conformational determinant. Replacement of the hCD97 RGD domain with RGE did not affect platelet adhesion or activation, indicating that CD97 signaling to platelets is not strictly RGD-dependent (Figures 1B, 1C, and S1B–S1D). Mouse CD97 does not contain an RGD tripeptide, and two isoforms of mouse CD97 stimulated platelet flattening and lamellipodia (Figures S1E and S1F). To determine whether CD97-initiated morphological activation requires platelet $\alpha_{IIb}\beta_3$ integrin, we incorporated eptifibatide into the adhesion assay. Eptifibatide (6 μM) inhibited CD97-dependent platelet flattening and lamellipodia formation but did not prevent platelet binding to purified CD97 (Figures 1B, 1C, S1C, S1D, S1F, and S1G), consistent with CD97 binding occurring prior to integrin activation. Blocking antibodies to $\alpha_5\beta_1$ or $\alpha_v\beta_3$ integrin had no effect upon platelet binding and activation (Figure S1D). These data identify a region within the extracellular domain of CD97 that can autonomously initiate $\alpha_{IIb}\beta_3$-dependent platelet activation.

CD97 Levels Influence Tumor Cell-Initiated Platelet Activation

To analyze the effect of CD97 membrane expression on the induction of platelet activation, we measured the ability of parental and CD97-depleted DU145/Ras prostate cancer cells (Figure 2A) to stimulate aggregation of washed, human platelets. Aggregation is dependent upon the initiation of platelet activation by tumor cells or added mediators such as thrombin (Figures 2B and 2C). Representative traces for parental, CD97-depleted, as well as CD97-depleted and subsequently reconstituted cells showed that CD97 depletion led to a decrease in tumor cell-induced platelet aggregation that was approximately similar to a 10-fold decrease in parental tumor cell concentration (Figure 2B). Eptifibatide noticeably slowed DU145/Ras-initiated platelet aggregation (Figure 2C), consistent with $\alpha_{IIb}\beta_3$-mediated amplification of platelet activation. By contrast, pre-incubation of platelets with aspirin, which inhibits the production of TXA2, a platelet autocrine stimulatory factor, had no effect on tumor cell-induced aggregation. We determined the levels of dense and α granule secretion using ATP and PF4 as markers, respectively, in supernatants of co-incubated DU145/Ras and platelets. As shown in Figure 2D, ATP and PF4 levels were induced by parental tumor cells. These levels were relatively lower following activation by tumor cells depleted for CD97, an activity that was reconstituted with ectopic CD97 expression. The presence of eptifibatide but not aspirin in the tumor-platelet incubations resulted in reduced PF4 and ATP in the platelet releasate. We conclude that CD97 expressed on tumor cells displays a platelet activating function.

Platelet Binding Initiates CD97/LPAR Heterodimer-Dependent Signaling in Tumor Cells

Platelets are a major source of serum LPA (Eichholtz et al., 1993) and CD97 is known to interact with LPAR1 and amplify LPA-dependent signaling via $G_{\alpha}12/13$ to RHO (Ward et al., 2011). To address the hypothesis that platelet interaction with CD97 initiates LPA-dependent RHO activation, we assayed RHO-GTP in DU145/Ras metastatic human prostate cancer cells (Yin et al., 2007) and mouse mammary carcinoma cells (Mvt-1) (Pei et al., 2004) following treatment with human platelets. RHO-GTP levels in both cell lines increased rapidly upon exposure to platelets in parental but not CD97-depleted cells (Figure 3A).

We previously determined using *in situ* proximity ligation analysis that CD97 and LPAR1 form complexes in cells (Ward et al., 2011). To analyze the regions of CD97 that associate with LPAR, we assayed the physical association of HA-tagged LPAR1 and either full-length CD97, a CD97 fragment consisting of the NTF domain anchored by the first transmembrane segment (referred to as NTF/TM1), or a MYC epitope-tagged fragment encoding the CTF, which represents the functional GPCR domain (Figure S2A). Immunoprecipitation of either LPAR1 or CD97 demonstrated that both the NTF/TM1 and CTF fragments interacted with LPAR1 (Figure S2B). This suggests that the CD97-LPAR1 interaction involves multiple contacts, or alternatively, that the overlapping region between the two CD97 constructs, the region between the membrane proximal proteolytic site and carboxyl terminus of the first transmembrane segment, is sufficient for interaction with LPAR1.

To investigate receptors on tumor cells that mediate plateletinitiated RHO activation, we used an SRE-luciferase reporter (Fromm et al., 1997) in RWPE-1 cells, which were depleted for CD97 to minimize the effects of endogenous CD97. As shown in the left panel of Figure 3B, RHO activity in the absence and presence of platelets was predominantly dependent upon CD97. Transient expression of full-length CD97 (FL-3E) or the NTF/TM1 fragment demonstrated constitutive RHO activation (Figure 3B), implying the occurrence of NTF/TM1 protein heterodimerization with a signal-transducing receptor. As described previously, the CD97 GPCR subunit (CTF) showed constitutive activity that was higher than the full-length receptor (Ward et al., 2011), suggesting an auto-inhibitory function of the extra-cellular domain (Langenhan et al., 2013). The reporter activity for FL and NTF/TM1 fragments, but not the CTF, increased in the presence of platelets. The constitutive and platelet-dependent signaling was partially inhibited by Ki16425, an LPAR-1, -2, and -3 inhibitor showing that CD97 NTF-dependent, plateletinitiated signaling is mediated significantly through LPARs. In addition, LPAR, but not CD97 CTF, activity was inhibited by Ki16425, implying that CTF alone does not lead to LPAR-dependent RHO signaling.

We asked whether RHO signaling was functionally linked to cellular invasion. Prior treatment with platelets for 16 hr increased invasion of DU145/Ras (Figure 3C) and Mvt-1 (Figure S2C) to 5% fetal calf serum (FCS), which contains LPA. CD97-depleted cells displayed decreased invasiveness to FCS that was not stimulated by prior incubation with platelets. Platelet priming of invasiveness paralleled RHO signaling in that the CD97 NTF/TM1 fragment was necessary and sufficient (Figure 3C), and priming was inhibited by the LPAR antagonist Ki16425 (Figures 3C and S2C). To address the specificity of platelet-primed invasion, we compared invasion toward LPA and EGF, chemotactic components in

serum (Figure 3D). Invasion to LPA, but not EGF, was stimulated by exposure to platelets and was CD97-dependent. As shown by maintenance of EGF-stimulated invasion, CD97 depletion did not have a non-specific inhibitory effect upon invasive ability. Thus, platelets stimulated invasion through a CD97-LPAR-dependent mechanism. The presence of eptifibatide during platelet-tumor cell exposure had no effect on RHO reporter activity (Figure 3E) or upon platelet-stimulated invasion (Figures 3F and S2D), suggesting that CD97/ LPAR signaling occurred independently of platelet morphological activation.

Others have shown that exposure of tumor cells to platelets for 40 hr leads to TGF-β release, one consequence of which is tumor cell epithelial to mesenchymal transition (EMT) and increased invasion (Labelle et al., 2011). We observed for DU145/Ras cells that EMT was evident at 40 but not 16 hr after platelet exposure and that increased pSMAD2 induction, decreased CDH1, and EMT appeared to be CD97 independent (Figure S2E). To investigate whether CD97-dependent invasion was influenced by TGF-β, we added 25 μM ALK5 inhibitor (SB431542) during the 16 hr incubation of platelets with DU145/Ras cells prior to the invasion assay. The majority of the platelet-induced increase in chemotaxis was not dependent upon TGF-β (Figure S2F). These data suggest that CD97/LPAR-dependent signaling mediates the majority of initial platelet-stimulated invasion, while TGF-β-dependent signaling develops more slowly.

CD97-Platelet Interactions Lead to $\alpha_{IIb}\beta_3$-Dependent Endothelial Cell Tight Junction Disruption

The interaction of platelets and tumor cells promotes transendothelial migration (TEM) (Schumacher et al., 2013). To establish whether CD97 may play a role in TEM of tumor cells, we assayed tumor cell migration through an endothelial monolayer of HUVECs by parental and CD97-depleted DU145/Ras cells in the presence of platelets. TEM, which requires both endothelial cell tight junction disruption and tumor cell migration, was stimulated by platelets in a CD97-dependent manner (Figure 4A). The interaction of DU145/Ras or Mvt-1 tumor cells with platelets led to the release of ATP (Figures 2D and 4B, respectively), the levels of which were dependent upon tumor cell CD97 expression. The addition of ATP-gS was sufficient to induce discontinuous junctions in human vein endothelial cells (HUVEC) (Figure S3A). Platelets were incubated with parental or CD97-depleted tumor cells and the cell-free supernatants generated from such incubations were used to treat HUVECs, which subsequently were assayed for cell-cell junctions as measured by the pattern of VE-Cadherin staining (Figures 4C, S3B, and S3C). Supernatants from platelets incubated with DU145/Ras cells (Figures 4D and S3D) or Mvt-1 cells (Figure 4E) potentiated dissociation of endothelial tight junctions, but supernatants from platelets exposed to CD97-depleted cells lacked this activity. Consistent with the ability of purified CD97 NTF to activate platelets morphologically, full-length or NTF/TM1–3E expression in CD97-depleted DU145/ Ras led to the release of endothelial disrupting mediators following incubation with platelets (Figure 4D). To investigate whether ATP was a source of soluble junction dissociation activity resulting from tumor-platelet interaction, we added apyrase during incubation of supernatants with endothelial cells, which demonstrated that ATP is necessary for the opening of the endothelial barrier (Figure 4F). We addressed the signaling mechanisms mediating release and found that the presence of eptifibatide, but not Ki16425

or aspirin during platelet-tumor cell interactions, strongly inhibited the generation of supernatants with endothelial tight junction dissociation activity (Figures 4E, 4G, and S3D). These data show that CD97 promotes tumor cell-induced platelet release of soluble endothelial disrupting activity, dependent upon $\alpha_{IIb}\beta_3$ integrin-mediated platelet activation but independent of LPAR signaling. ATP was a necessary and sufficient mediator of endothelial junction disruption (Figures 4F and S3A), and the presence of ATP in supernatants from tumor-platelet incubations correlated with the presence of CD97 on tumor cells (Figures 2D and 4B).

CD97-Platelet Interactions Promote *In Vivo* TEM and Experimental Metastasis

CD97-dependent tumor cell-platelet interactions contribute to both tumor cell invasion (Figure 3F) and endothelial junction disruption (Figures 4D and 4E). To confirm these activities in TEM, tumor cells and platelets were seeded directly into TEM chambers in the absence and presence of inhibitors that decreased LPAR signaling (Ki16425) or $\alpha_{IIb}\beta_3$ integrin ligation (eptifibatide). Importantly, TEM of tumor cells was inhibited by the presence of either drug (Figures 5A and 5B). Apyrase also diminished the platelet-dependent increase in transendothelial migration indicating a role for ATP (Figure S4A). Consistent with the CD97 structural requirements for platelet-tumor interaction and activation, TEM was reconstituted in CD97-depleted DU145/Ras cells with either CD97 FL-3E or the NTF/TM1–3E fragment expression (Figure S4B). To determine whether CD97 on tumor cells affected vascular permeability *in vivo*, we analyzed the extent to which Evans blue permeated lung tissue following tail vein inoculation of parental and CD97-depleted Mvt-1 cells into syngeneic hosts. Macroscopic examination and subsequent quantification of extracted Evans blue were performed (Figure 5C). 24 hr post inoculation, lungs from animals receiving parental cells were significantly more permeable than those from animals receiving CD97-depleted cells. The specificity of CD97-depletion was demonstrated by the ability to reconstitute vascular permeability with ectopic expression of CD97 in CD97-depleted cells. Taken together, these *in vitro* and *in vivo* data support a role for CD97 in transendothelial invasion (Figure 5D). To further assess whether *in vivo* tumor cell extravasation and growth was altered upon CD97-platelet interactions, pulmonary metastatic foci were quantified 14 days following tail vein injection of Mvt-1 cells. Parental and CD97-depleted mouse mammary Mvt-1 cells were incubated with buffer or platelets for 20 hr prior to intravenous injection into FVB/NJ mice. CD97 depletion strongly inhibited metastasis formation overall (Figure 5E). The number of metastatic lesions was significantly greater when Mvt-1 cells were pretreated with platelets, although for CD97-depleted cells, incubation with platelets no longer demonstrated a stimulatory effect. Similarly, in a human xenograft bone metastasis model, when DU145/Ras prostate cells were inoculated via an intracardiac route, depletion of CD97 significantly inhibited metastasis. The number of bone metastases increased as a result of platelet exposure prior to injection, but in CD97-depleted cells, platelet incubation no longer increased metastasis (Figures S4C and S4D). These results demonstrate that metastatic competence is influenced by CD97 expression, and platelet priming, leading to enhanced metastatic colonization, is CD97-dependent.

CD97 Non-redundantly Promotes Thyroid Cancer Invasion and Metastasis in a Genetically Engineered Mouse Model

To analyze the consequences of CD97 loss on an endogenously initiated progressive cancer, we used *Thrb*$^{PV/PV}$ mice, an established model in which mice spontaneously develop thyroid carcinomas of follicular cells with pathologic progression similar to human thyroid follicular cell tumorigenesis (Kaneshige et al., 2000). CD97 overexpression promotes vascular invasion and lung metastasis in this model (Ward et al., 2013), consistent with high CD97 expression in progressive clinical thyroid cancer. Here, we investigated the impact of germline CD97 loss. Earlier analyses of CD97 null mice demonstrated mild granulocytosis without other apparent phenotypes, including no overt abnormalities associated with inflammation or hematopoietic development (Wang et al., 2007). In addition, CD97 is expressed on platelets, but as shown in Figure 6A, loss of CD97 did not influence activated platelet aggregation. Loss of CD97 in this mouse model (Figure 6B) did not affect primary tumor growth (Figure 6C); however, the rate for development of vascular invasion and metastasis was notably slowed (Figure 6D). There were highly statistically significant differences in comparing the relative vascular invasion and metastasis for CD97$^{+/+}$ and CD97$^{-/-}$ mice as measured in cohorts at early time points (29–44 weeks) as well as in cohorts analyzed during the entirety of cancer progression (29–66 weeks) (Figure 6E). These data show that in a progressive thyroid cancer model, loss of CD97 decreased extravasation and metastasis, which may result from contributions of tumor and/or microenvironmental CD97.

Prostate Cancer Circulating Tumor Cells and Metastases Express CD97

CD97 protein overexpression has been reported in various malignancies in studies encompassing small to comprehensive sample sizes (Liu et al., 2012; Safaee et al., 2013; Ward et al., 2011, 2013). To take advantage of the extensive cohorts available as TCGA datasets, we compared CD97 transcript levels in epithelial cancers and normal tissue (Figure S5). Several cancer types demonstrate a distribution in cancer versus normal with increased median expression as well as a significantly disproportionate number of cases within the upper quartile. Bladder and lung cancers did not show increased expression compared to normal that may be due in part to CD97 expression in normal non-epithelial cells, i.e., smooth muscle and alveolar macrophages, respectively (Jaspars et al., 2001). These data confirm and extend the observations that CD97 is widely overexpressed in epithelial malignancies.

If CD97 plays a role in potentiating tumor cell dissemination via extravasation at distal organs, one would predict detectable CD97 expression on at least a proportion of circulating tumor cells (CTCs) and metastatic lesions. Here, we analyzed CD97 expression in clinical prostate cancer metastases and CTCs. We previously demonstrated that CD97 is expressed in ~60% of primary prostate cancers (Ward et al., 2011), and as shown in Figure 7A, CD97 is expressed in a majority of prostate cancer soft tissue metastases and more strongly and uniformly in bone metastases. CD97 was present at variable levels in CTCs captured from the blood of 25 patients with metastatic prostate cancer (Figures 7B–7D). Interestingly, there was a subset of patients (1–9, ~35%) showing predominantly intermediate and high CD97 expression in their CTCs (Figures 7C and 7D).

DISCUSSION

During hematogenous dissemination, platelets interact with tumor cells leading to platelet activation and release of soluble mediators that alter the phenotype of the tumor cells and surrounding host cells (Labelle and Hynes, 2012). Although physiologically important events distal to tumor cell-platelet interactions such as TEM and invasiveness have been described (Labelle and Hynes, 2012; Schumacher et al., 2013), the proximal events, which initiate platelet activation, are incompletely characterized. We identify a role for the adhesion GPCR CD97 in activating platelets. Of particular interest is the additional activity of tumor CD97 as a motility receptor for LPA released from platelets. One result of CD97 binding to platelets would be to concentrate platelet-derived LPA in proximity to CD97-LPAR heterodimers to induce RHO signaling, producing an invasive phenotype. Simultaneously, platelet activation leads to granule release and consequent dissociation of the endothelial barrier, thereby coupling the timing of tumor cell motility to endothelial barrier disruption (Figure 5D). Consistent with TEM assays, we observed CD97-dependence for tumor cell induced *in vivo* vascular permeability and platelet-enhanced metastasis in preclinical models.

Here, we demonstrate that purified CD97 extracellular region autonomously activates platelets. Immobilized CD97 binds washed, resting platelets and stimulates spreading and clustering, indicators of $\alpha_{IIb}\beta_3$ signaling (Shen et al., 2013). The CD97 receptor on platelets is yet to be determined. The presence of blocking antibodies to $\alpha_5\beta_1$ or $\alpha_v\beta_3$ did not inhibit platelet binding or morphological activation (Figure S1D), suggesting that these integrin receptors are not necessary for CD97-induced platelet activation. Another ligand, CD55, is limited to species-specific binding (Hamann et al., 1996), while we observed cross species CD97-dependent platelet activation. It is possible that CD97 directly binds $\alpha_{IIb}\beta_3$, similarly to fibronectin (McCarty et al., 2004). However, the dispensability of the CD97 RGD sequence for platelet binding and the occurrence of platelet binding in the presence of eptifibatide makes it more likely that $\alpha_{IIb}\beta_3$ activation occurs in response to CD97-induced platelet signaling, secretion of platelet granule contents, and the subsequent activation cascade.

CD97 is usually undetectable in normal tissues outside the hematopoietic system and smooth muscle (Jaspars et al., 2001), but remarkably, is abnormally expressed in a wide array of common solid tumors including prostate, gastric, colorectal, thyroid, renal, and esophageal, among others (Figure S5) (Aust et al., 2002; Steinert et al., 2002; Ward et al., 2011, 2013). How is a tumor-associated antigen able to initiate platelet activation while normal cells expressing seemingly the same protein do not? We hypothesize that normal tissues (such as CD97-expressing neutrophils) have mechanisms to inhibit platelet activation. These mechanisms may be direct and related to the structure of CD97 or associated proteins, or alternatively, may be indirect through the expression of platelet inhibitory factors, exemplified by endothelial cell prostacyclins. Other cell surface antigens, expressed on both tumor and normal cells, can serve as adhesive receptors for platelets including the following tumor:platelet pairs: podoplanin:CLEC2 (Kato et al., 2008), sialyl $Lewis^X$:P-selectin (Borsig et al., 2002), and HMGB1:TLR4 (Yu et al., 2014).

Indirect evidence from LMW heparin and aspirin clinical trials suggests that disrupting tumor cell-platelet cross-talk may have efficacy for preventing or treating early metastatic disease (Erpenbeck and Schön, 2010; Labelle and Hynes, 2012). Pharmacologic treatments to inhibit platelet activation are one promising approach, but also have the potential to effect normal hemostatic and thrombotic functions (Gresele et al., 2017). A novel strategy is to target CD97 to disrupt platelet tumor cell interactions, decreasing tumor cell dissemination. In theory, such an approach could be useful in additional studies are needed, the demonstration here of high CD97 expression on CTCs from patients with metastatic prostate cancer and previous studies showing that CD97 is highly expressed on invasive thyroid cancer (Ward et al., 2013) suggest that blocking CD97 in progressive disease may be useful. One question is the potential toxicities associated with such an approach. The normal functions of CD97 are not known, and germline loss of CD97 leads to a mild granulopoiesis with no apparent loss of immunological function (Wang et al., 2007). Nevertheless, effective therapeutic blocking may be determined by achieving specificity for modulating CD97 functions in tumor verses normal cells.

In summary, CD97 coordinates the coincidence of tumor cell migration and endothelial barrier retraction as a result of rapid bidirectional signaling between tumor cells and platelets. In addition, CD97 is overexpressed in a variety of tumor types and is necessary for efficient metastasis in pre-clinical models. Tumor CD97 represents a previously unappreciated participant in platelet-mediated effects upon cancer progression.

EXPERIMENTAL PROCEDURES

Platelet Adhesion

CD97 protein purification and platelet preparation are detailed in the Supplemental Experimental Procedures. 15 μL soluble protein (10 μg/mL) was spotted on the surface of a 35-mm glass bottom dish (MatTek) and incubated overnight at 4°C. Plates were blocked 1 hr with PBS/1% BSA. Following a Tyrode's buffer (TB) rinse, 200 μL of platelets ($3\ 3\ 10^7$) with or without 6 μm eptifibatide were added to each plate and incubated for 45 min at 37°C. Following two PBS rinses, adhered platelets were fixed for 12 min with 4% PFA, blocked in PBS/20% goat serum/1%BSA for 15 min, and stained with Rhodamine-Phalloidin diluted (1:40) in PBS/2% goat serum/1%BSA for 1 hr.

Endothelial Cellular Junctions and TEM

Visualization of the endothelial barrier and TEM assays were done as previously described (Schumacher et al., 2013) with modifications detailed in the Supplemental Experimental Procedures.

Experimental Metastasis Models

Patient CTCs were collected under a University of Wisconsin IRB approved protocol. All animal care and studies were performed in accordance with a protocol approved by the NIH Animal Care and Use Committee. Mvt-1 metastasis assays were performed as described previously (Faraji et al., 2012). 2×10^7 Mvt-1 cells were treated with ~2×10^9 platelets in media for 20 hr prior to tail vein injection. The H&E stained lung sections were imaged

using an Aperio CS Slide Scanner with a 203 lens and the number of metastatic foci was counted using ScanScope software. DU145/Ras bone metastasis assays were performed, analyzed, and scored as described previously (Liu et al., 2015). 2×10^7 DU145/Ras cells were treated with ~2 3 10^9 platelets in media for 20 hr prior to intracardiac injection.

Vascular Permeability Assay

1×10^6 Mvt-1 tumor cells were injected intravenously into the tail vein of female FVB/NJ mice. After 24 hr, 20 mg/kg of Evans blue dye (EB) in PBS was injected via tail vein, followed by euthanasia 30 min later. The lungs were perfused with PBS, dissected, weighed, and homogenized in 5 vol of formamide. EB was extracted with an 18 hr incubation at 60°C, and the absorption was measured at 620 nm and corrected for the presence of heme pigments. The EB concentration in the lung homogenates was calculated against a standard curve (mgrams Evans blue dye/ g lung tissue).

Statistical Analysis

All data shown is representative of at least 3 independent experiments. Statistical analyses were performed using Prism software. Mean values shown are ± SD or SEM as indicated in the figure legends. Statistical significance was determined by unpaired two-tailed t test and is designated as *p < 0.05; **p < 0.01; ***p < 0.001; ****p < 0.0001; NS, not significant.

Additional methods are contained in the Supplemental Experimental Procedures.

Supplementary Material

Refer to Web version on PubMed Central for supplementary material.

ACKNOWLEDGMENTS

The authors wish to thank Subhadra Banerjee of the CCR FACS Core Facility, Seth Steinberg for statistical advice, Colm Morrissey and Eva Corey for meta-static prostate cancer TMAs, and the UWCCC GU clinical research group especially Jamie Wiepz, Jill Kubiak, Mulusew Yayehyirad, Dorothea Horvath, and Mary Jane Staab. We would also like to thank all of the patients who participated in this study. This research was supported by the Intramural Research Program of the NIH, National Cancer Institute, Center for Cancer Research, by grants from the Movember-Prostate Cancer Foundation Challenge Award, NIH (1R01CA181648), DOD PCRP (W81XWH-12-1-0052), and a Prostate Cancer Foundation Young Investigator award to J.L.

REFERENCES

Amirkhosravi A, Mousa SA, Amaya M, Blaydes S, Desai H, Meyer T, and Francis JL (2003). Inhibition of tumor cell-induced platelet aggregation and lung metastasis by the oral GpIIb/IIIa antagonist XV454. Thromb. Haemost 90, 549–554. [PubMed: 12958625]

Araç D, Boucard AA, Bolliger MF, Nguyen J, Soltis SM, Südhof TC, and Brunger AT (2012). A novel evolutionarily conserved domain of cell-adhesion GPCRs mediates autoproteolysis. EMBO J 31, 1364–1378. [PubMed: 22333914]

Aust G, Steinert M, Schütz A, Boltze C, Wahlbuhl M, Hamann J, and Wobus M (2002). CD97, but not its closely related EGF-TM7 family member EMR2, is expressed on gastric, pancreatic, and esophageal carcinomas. Am.J. Clin. Pathol 118, 699–707.

Borsig L, Wong R, Hynes RO, Varki NM, and Varki A (2002). Synergistic effects of L- and P-selectin in facilitating tumor metastasis can involve non-mucin ligands and implicate leukocytes as enhancers of metastasis. Proc. Natl. Acad. Sci. USA 99, 2193–2198. [PubMed: 11854515]

Boucharaba A, Serre CM, Grès S, Saulnier-Blache JS, Bordet JC, Guglielmi J, Clézardin P, and Peyruchaud O (2004). Platelet-derived lysophosphatidic acid supports the progression of osteolytic bone metastases in breast cancer. J. Clin. Invest 114, 1714–1725. [PubMed: 15599396]

Eichholtz T, Jalink K, Fahrenfort I, and Moolenaar WH (1993). The bioactive phospholipid lysophosphatidic acid is released from activated platelets. Biochem. J 291, 677–680. [PubMed: 8489494]

Erpenbeck L, and Schön MP (2010). Deadly allies: the fatal interplay between platelets and metastasizing cancer cells. Blood 115, 3427–3436. [PubMed: 20194899]

Faraji F, Pang Y, Walker RC, Nieves Borges R, Yang L, and Hunter KW (2012). Cadm1 is a metastasis susceptibility gene that suppresses metastasis by modifying tumor interaction with the cell-mediated immunity. PLoS Genet 8, e1002926. [PubMed: 23028344]

Fromm C, Coso OA, Montaner S, Xu N, and Gutkind JS (1997). The small GTP-binding protein Rho links G protein-coupled receptors and Galpha12 to the serum response element and to cellular transformation. Proc. Natl. Acad. Sci. USA 94, 10098–10103. [PubMed: 9294169]

Gasic GJ, Gasic TB, and Stewart CC (1968). Antimetastatic effects associated with platelet reduction. Proc. Natl. Acad. Sci. USA 61, 46–52. [PubMed: 5246932]

Gresele P, Momi S, Malvestiti M, and Sebastiano M (2017). Platelet-targeted pharmacologic treatments as anti-cancer therapy. Cancer Metastasis Rev 36, 331–355. [PubMed: 28707198]

Hamann J, Vogel B, van Schijndel GM, and van Lier RA (1996). The seven-span transmembrane receptor CD97 has a cellular ligand (CD55, DAF). J. Exp. Med 184, 1185–1189. [PubMed: 9064337]

Hynes RO (2002). Integrins: bidirectional, allosteric signaling machines. Cell 110, 673–687. [PubMed: 12297042]

Im JH, Fu W, Wang H, Bhatia SK, Hammer DA, Kowalska MA, and Muschel RJ (2004). Coagulation facilitates tumor cell spreading in the pulmonary vasculature during early metastatic colony formation. Cancer Res 64, 8613–8619. [PubMed: 15574768]

Jaspars LH, Vos W, Aust G, Van Lier RA, and Hamann J (2001). Tissue distribution of the human CD97 EGF-TM7 receptor. Tissue Antigens 57, 325–331. [PubMed: 11380941]

Jin J, Mao Y, Thomas D, Kim S, Daniel JL, and Kunapuli SP (2009). RhoA downstream of G(q) and G(12/13) pathways regulates protease-activated receptor-mediated dense granule release in platelets. Biochem. Pharmacol 77, 835–844. [PubMed: 19073150]

Kaneshige M, Kaneshige K, Zhu X, Dace A, Garrett L, Carter TA, Kazlauskaite R, Pankratz DG, Wynshaw-Boris A, Refetoff S, et al. (2000). Mice with a targeted mutation in the thyroid hormone beta receptor gene exhibit impaired growth and resistance to thyroid hormone. Proc. Natl. Acad. Sci. USA 97, 13209–13214. [PubMed: 11069286]

Kato Y, Kaneko MK, Kunita A, Ito H, Kameyama A, Ogasawara S, Matsuura N, Hasegawa Y, Suzuki-Inoue K, Inoue O, et al. (2008). Molecular analysis of the pathophysiological binding of the platelet aggregation-inducing factor podoplanin to the C-type lectin-like receptor CLEC-2. Cancer Sci 99, 54–61. [PubMed: 17944973]

Labelle M, and Hynes RO (2012). The initial hours of metastasis: the importance of cooperative host-tumor cell interactions during hematogenous dissemination. Cancer Discov 2, 1091–1099. [PubMed: 23166151]

Labelle M, Begum S, and Hynes RO (2011). Direct signaling between platelets and cancer cells induces an epithelial-mesenchymal-like transition and promotes metastasis. Cancer Cell 20, 576–590. [PubMed: 22094253]

Langenhan T, Aust G, and Hamann J (2013). Sticky signaling–adhesion class G protein-coupled receptors take the stage. Sci. Signal 6, re3. [PubMed: 23695165]

Leblanc R, Lee SC, David M, Bordet JC, Norman DD, Patil R, Miller D, Sahay D, Ribeiro J, Clézardin P, et al. (2014). Interaction of plateletderived autotaxin with tumor integrin aVb3 controls metastasis of breast cancer cells to bone. Blood 124, 3141–3150. [PubMed: 25277122]

Liu D, Trojanowicz B, Ye L, Li C, Zhang L, Li X, Li G, Zheng Y, and Chen L (2012). The invasion and metastasis promotion role of CD97 small iso-form in gastric carcinoma. PLoS ONE 7, e39989. [PubMed: 22768192]

Liu YN, Yin J, Barrett B, Sheppard-Tillman H, Li D, Casey OM, Fang L, Hynes PG, Ameri AH, and Kelly K (2015). Loss of androgen-regulated microRNA 1 activates SRC and promotes prostate cancer bone metastasis. Mol. Cell. Biol 35, 1940–1951. [PubMed: 25802280]

McCarty OJ, Zhao Y, Andrew N, Machesky LM, Staunton D, Frampton J, and Watson SP (2004). Evaluation of the role of platelet integrins in fibronectin-dependent spreading and adhesion. J. Thromb. Haemost 2, 1823–1833. [PubMed: 15456495]

Millard M, Odde S, and Neamati N (2011). Integrin targeted therapeutics. Theranostics 1, 154–188. [PubMed: 21547158]

Nieswandt B, Hafner M, Echtenacher B, and Männel DN (1999). Lysis of tumor cells by natural killer cells in mice is impeded by platelets. Cancer Res 59, 1295–1300. [PubMed: 10096562]

Palumbo JS, Talmage KE, Massari JV, La Jeunesse CM, Flick MJ, Kombrinck KW, Jirousková M, and Degen JL (2005). Platelets and fibrin(ogen) increase metastatic potential by impeding natural killer cell-mediated elimination of tumor cells. Blood 105, 178–185. [PubMed: 15367435]

Pei XF, Noble MS, Davoli MA, Rosfjord E, Tilli MT, Furth PA, Russell R, Johnson MD, and Dickson RB (2004). Explant-cell culture of primary mammary tumors from MMTV-c-Myc transgenic mice. In Vitro Cell. Dev. Biol. Anim 40, 14–21. [PubMed: 15180438]

Petersen SC, Luo R, Liebscher I, Giera S, Jeong SJ, Mogha A, Ghidinelli M, Feltri ML, Schöneberg T, Piao X, and Monk KR (2015). The adhesion GPCR GPR126 has distinct, domain-dependent functions in Schwann cell development mediated by interaction with laminin-211. Neuron 85, 755–769. [PubMed: 25695270]

Safaee M, Clark AJ, Ivan ME, Oh MC, Bloch O, Sun MZ, Oh T, and Parsa AT (2013). CD97 is a multifunctional leukocyte receptor with distinct roles in human cancers (Review). Int. J. Oncol 43, 1343–1350. [PubMed: 23969601]

Schumacher D, Strilic B, Sivaraj KK, Wettschureck N, and Offermanns S (2013). Platelet-derived nucleotides promote tumor-cell transendothelial migration and metastasis via P2Y2 receptor. Cancer Cell 24, 130–137. [PubMed: 23810565]

Shen B, Zhao X, O'Brien KA, Stojanovic-Terpo A, Delaney MK, Kim K, Cho J, Lam SC, and Du X (2013). A directional switch of integrin signalling and a new anti-thrombotic strategy. Nature 503, 131–135. [PubMed: 24162846]

Stacey M, Chang GW, Davies JQ, Kwakkenbos MJ, Sanderson RD, Hamann J, Gordon S, and Lin HH (2003). The epidermal growth factor- like domains of the human EMR2 receptor mediate cell attachment through chondroitin sulfate glycosaminoglycans. Blood 102, 2916–2924. [PubMed: 12829604]

Stegner D, Dütting S, and Nieswandt B (2014). Mechanistic explanation for platelet contribution to cancer metastasis. Thromb. Res 133 (Suppl 2), S149–S157. [PubMed: 24862136]

Steinert M, Wobus M, Boltze C, Schütz A, Wahlbuhl M, Hamann J, and Aust G (2002). Expression and regulation of CD97 in colorectal carcinoma cell lines and tumor tissues. Am. J. Pathol 161, 1657–1667. [PubMed: 12414513]

Wandel E, Saalbach A, Sittig D, Gebhardt C, and Aust G (2012). Thy-1 (CD90) is an interacting partner for CD97 on activated endothelial cells.J. Immunol 188, 1442–1450. [PubMed: 22210915]

Wang T, Ward Y, Tian L, Lake R, Guedez L, Stetler-Stevenson WG, and Kelly K (2005). CD97, an adhesion receptor on inflammatory cells, stimulates angiogenesis through binding integrin counterreceptors on endothelial cells. Blood 105, 2836–2844. [PubMed: 15576472]

Wang T, Tian L, Haino M, Gao JL, Lake R, Ward Y, Wang H, Sieben-list U, Murphy PM, and Kelly K (2007). Improved antibacterial host defense and altered peripheral granulocyte homeostasis in mice lacking the adhesion class G protein receptor CD97. Infect. Immun 75, 1144–1153. [PubMed: 17158902]

Ward Y, Lake R, Yin JJ, Heger CD, Raffeld M, Goldsmith PK, Merino M, and Kelly K (2011). LPA receptor heterodimerizes with CD97 to amplify LPA-initiated RHO-dependent signaling and invasion in prostate cancer cells. Cancer Res 71, 7301–7311. [PubMed: 21978933]

Ward Y, Lake R, Martin PL, Killian K, Salerno P, Wang T, Meltzer P, Merino M, Cheng SY, Santoro M, et al. (2013). CD97 amplifies LPA receptor signaling and promotes thyroid cancer progression in a mouse model. Oncogene 32, 2726–2738. [PubMed: 22797060]

Yin J, Pollock C, Tracy K, Chock M, Martin P, Oberst M, and Kelly K (2007). Activation of the RalGEF/Ral pathway promotes prostate cancer metastasis to bone. Mol. Cell. Biol 27, 7538–7550. [PubMed: 17709381]

Yu LX, Yan L, Yang W, Wu FQ, Ling Y, Chen SZ, Tang L, Tan YX, Cao D, Wu MC, et al. (2014). Platelets promote tumour metastasis via interaction between TLR4 and tumour cell-released high-mobility group box1 protein. Nat. Commun 5, 5256. [PubMed: 25348021]

Highlights

- The adhesion GPCR CD97 is a tumor antigen that directly activates platelets
- CD97-platelet interactions coordinate tumor invasion and endothelial cell retraction
- Tumor CD97 is required for vascular invasion and metastasis in pre-clinical models
- CD97 is expressed in several primary and metastatic cancer types and in CTCs

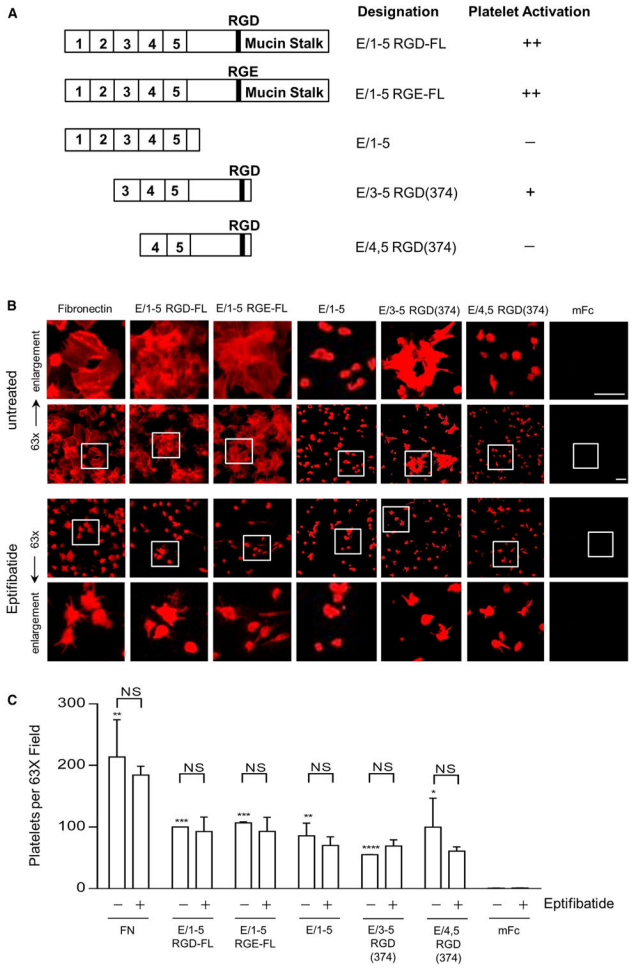

Figure 1. Adhesion to CD97 Activates Platelets

(A) Fusion constructs with mouse Fc (mFc) that were used to generate purified CD97 are shown without the Fc region. Constructs designated as full-length (FL) include the extracellular domain of CD97 up to the natural proteolysis processing site at amino acid 531. The human CD97 isoform containing 5(E/1–5) EGF-like repeats, the RGD motif, and mucin stalk was used in adhesion studies along with the RGD to RGE and 3 different deletion mutants.

(B) Platelet morphology and relative adhesion to various forms of plastic-bound purified CD97 or mFc only in the absence and presence of eptifibatide (6 μM). Bound platelets were stained for F-actin (red) and confocal images (633 ×) were generated. Enlargements of areas in white boxes are shown above untreated panels and below eptifibatide-treated panels. Scale bars, 5 μM.

(C) The number of bound platelets per 633 microscopic field (n = 5) relative to FL CD97 was quantified. Error bars ± SEM. Plastic-bound mFc was used to determine statistical significance of platelet adhesion to CD97. *$p < 0.05$; **$p < 0.01$; ***$p < 0.001$; ****$p < 0.0001$; not significant (NS) were determined by unpaired t test. All results shown are representative of at least 3 independent experiments.

See also Figure S1.

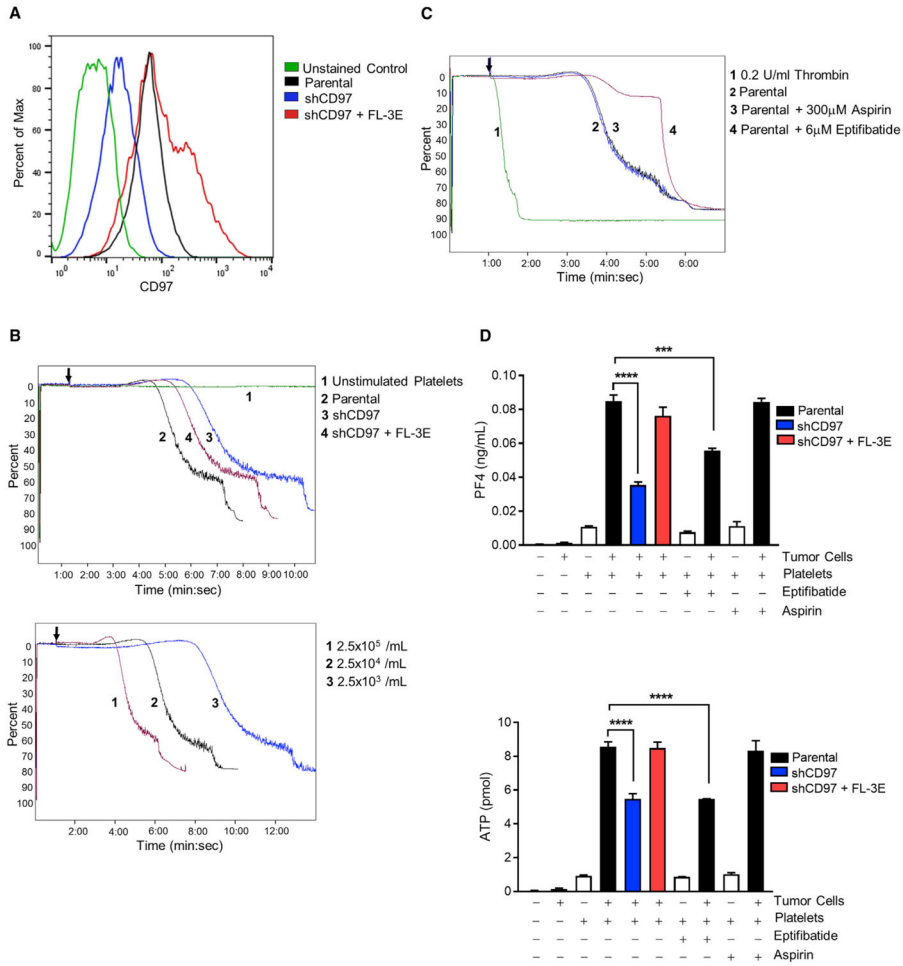

Figure 2. The Strength of Tumor Cell-Induced Platelet Activation Is Influenced by Tumor CD97 Levels

(A) Representative FACS tracings of CD97 in live cells including DU145/Ras: parental, CD97-depleted, and CD97-depleted and reconstituted.

(B) Top: representative aggregometer tracings for platelet aggregation following the addition 2.5×10^5 cells/mL of the indicated tumor cells, n = 5. Bottom: representative aggregometer tracings for platelet aggregation following the addition of the indicated numbers of parental DU145/Ras cells, n = 3. Bold arrows show the time of tumor cell addition (1 min).

(C) Representative aggregometer tracing for platelet aggregation following the addition of thrombin or DU145/Ras cells. Platelets were pre-treated with 300 μM aspirin or 6 μM eptifibatide as indicated. No aggregation was observed with platelets alone, n = 3.

(D) Release of PF4 (top) and ATP (bottom) from platelets alone, tumor cells alone, or a mixture of the indicated DU145/Ras tumor cells and platelets. Platelets were pre-treated with inhibitors as indicated. Values represent means of quadruplicates ± SEM; ***p < 0.001, ****p < 0.0001; n = 3.

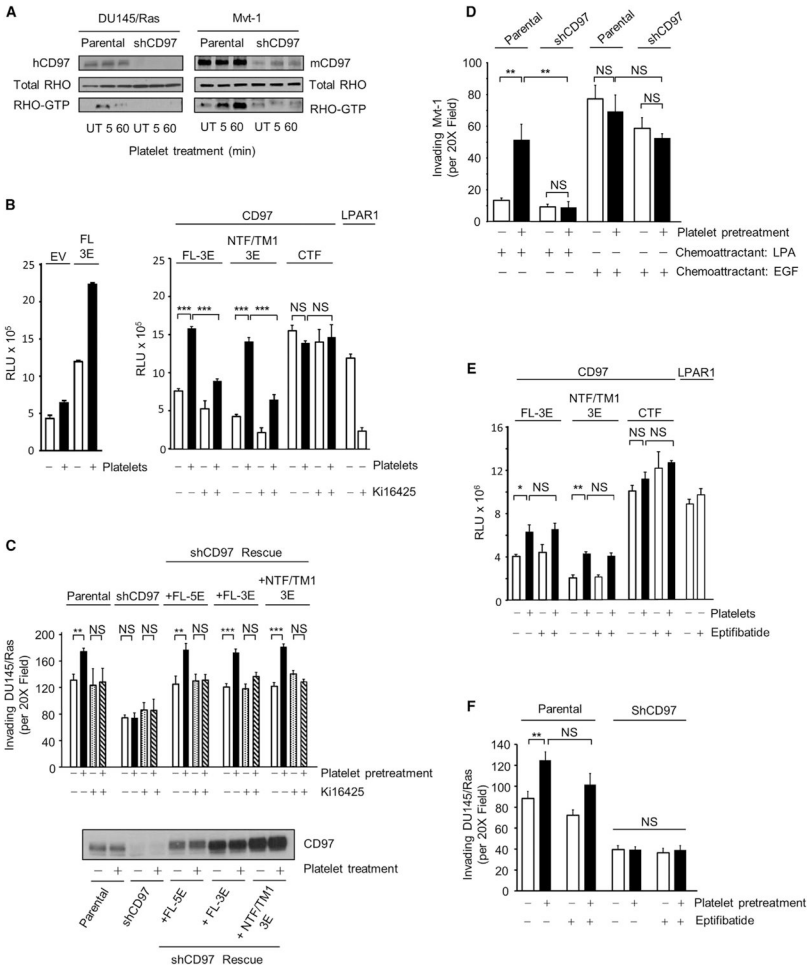

Figure 3. Platelets Stimulate Tumor Cell CD97/LPAR-Dependent Increased RHO Levels and Invasion

(A) Western blot analysis showing CD97, RHO, and RHO-GTP levels in DU145/Ras and Mvt-1 cells following platelet treatment for various times. Untreated (UT) cells were collected at 5 and 60 min following platelet buffer addition. No effect of buffer was observed, and the 5 min UT sample is shown.

(B) CD97-dependent RHO reporter activity following activation by platelets. RWPE1cells were transfected with the RHO-specific SRE-luciferase reporter and Renilla transfection control constructs along with the indicated CD97 expression plasmids encoding full-length, NTF/TM1, or CTF fragments. Left: absolute activity. Right: activity after background subtraction (i.e., no CD97 transfection). The SRE-luciferase reporter assay was conducted following incubation with buffer or platelets in the presence or absence of 20 mM Ki16425. Reporter activities represent the means ± SEM. All results shown are representative of at least 4 independent experiments.

(C) Top: DU145/Ras cells expressing CD97 (parental), depleted for CD97 (shCD97) or rescued with either full-length CD97 (FL-5E and FL-3E) or NTF/TM1–3E, tested for invasiveness to 5% FCS. Tumor cells were incubated with buffer or platelets in the presence or absence of Ki16425 (20 μM) for 16 hr prior to the assay. Bottom: western blot analysis of CD97 expression in the parental, silenced, and reconstituted DU145/Ras cell lines.

(D) Parental or CD97-depleted (shCD97) Mvt-1 treated with buffer or platelets for 16 hr were tested for invasiveness to LPA (10 μM) or EGF (25 ng/mL).
(E) CD97-dependent RHO reporter activity as described in (B) following activation by platelets in the presence or absence of 6 μM eptifibatide.
(F) Parental or CD97-depleted (shCD97) DU145/Ras cells were incubated with buffer or platelets in the presence or absence of eptifibatide (6 μM) for 16 hr prior to the invasion assay and allowed to invade to 5% FCS for 3.5 hr.
The p values for all panels were calculated by two-tailed unpaired t test. *$p < 0.05$; **$p < 0.01$; ***$p < 0.001$; ****$p < 0.0001$; NS, not significant.
See also Figure S2.

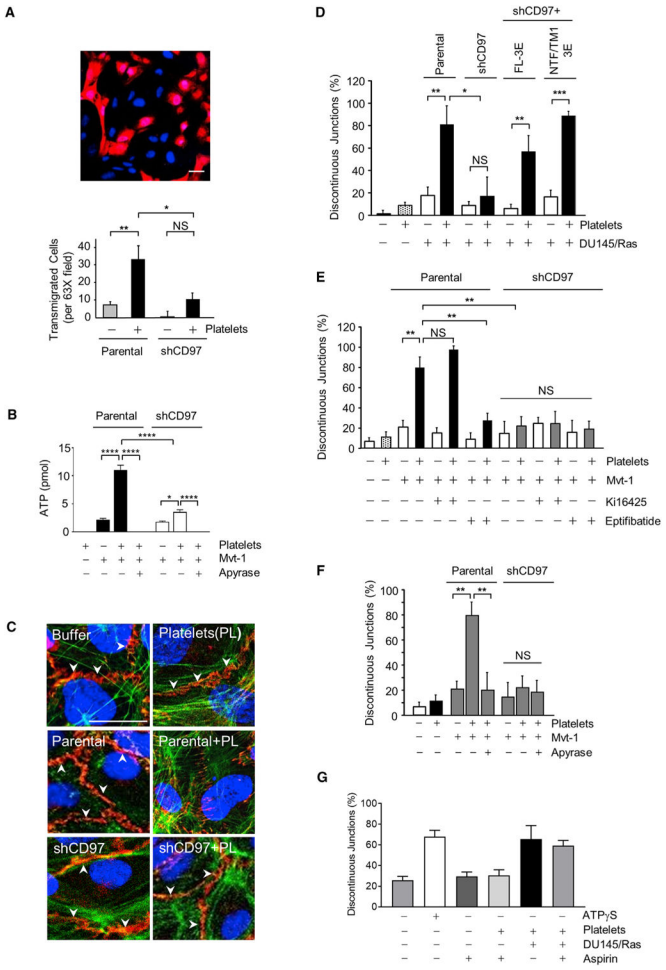

Figure 4. Tumor CD97 Stimulates Platelet $\alpha_{IIb}\beta_3$-Dependent Nucleotide Secretion Leading to Endothelial Junction Dissociation

(A) Transendothelial migration (TEM) of parental or CD97-depleted (shCD97) DU145/Ras cells in the absence or presence of platelets. Top: confocal image showing tumor cells stained with SNARF-1 (red) and unstained human umbilical vein endothelial cells (HUVEC) on the Transwell membrane. DAPI stain was used to identify nuclei. Scale bar, 5 μM. Bottom: relative TEM for parental or CD97-depleted DU145/Ras cells. All results shown are representative of at least 4 independent experiments. Error bars represent ± SEM.

(B) Relative levels of ATP released from platelets alone, Mvt-1 cells alone, or cells incubated with platelets. Parental and CD97-depleted (shCD97) cells were tested, and apyrase was added to selected supernatants as a control. Results shown are representative of 3 independent experiments. Shown are mean values of 5 replicates ± SD.

(C) Tight junctions of HUVEC incubated with only buffer or cell-free supernatants from platelets alone (PL), DU145/Ras cells alone (Parental), or incubated with platelets (Parental + PL). Parental cells and CD97-depleted cells (shCD97) were tested. Following treatment, HUVEC were stained for vascular endothelial (VE)-cadherin (red), F-actin (green), and cell nuclei (blue). Continuous cellular junctions are indicated with arrowheads. Scale bar, 5 μM.

(D) The percentage of discontinuous cellular junctions was quantified (n = 5) for buffer only and supernatants from platelets alone, DU145/Ras cells alone, and cells incubated with

platelets. The tumor cells used in this assay included parental and CD97-depleted (shCD97) as well as cells rescued with full-length CD97 (FL-3E) and NTF/TM1–3E.

(E) Mvt-1 tumor cells (parental and CD97-depleted) were incubated with platelets in the absence or presence of Ki16425 (20 μM) or eptifibatide (6 μM) and the resulting supernatants were assayed for junction disrupting activity. Results shown are representative of at least 3 independent experiments. Shown are means ± SD.

(F) Effect of apyrase on the percentage of discontinuous junctions induced by supernatants from Mvt-1 cells incubated with platelets. Parental and CD97-depleted (shCD97) Mvt-1 cells were used in the assay as indicated.

(G) The percentage of discontinuous cellular junctions was quantified (n = 5) after the addition of buffer with or without (300 μM) aspirin, supernatants from platelets alone incubated with aspirin, or platelets and DU145/Ras cells incubated in the presence and absence of aspirin.

The p values in (A), (B), (D), (E), and (F) were calculated by two-tailed unpaired t test. *$p < 0.05$; **$p < 0.01$; ***$p < 0.001$; ****$p < 0.0001$; NS, not significant.

See also Figure S3.

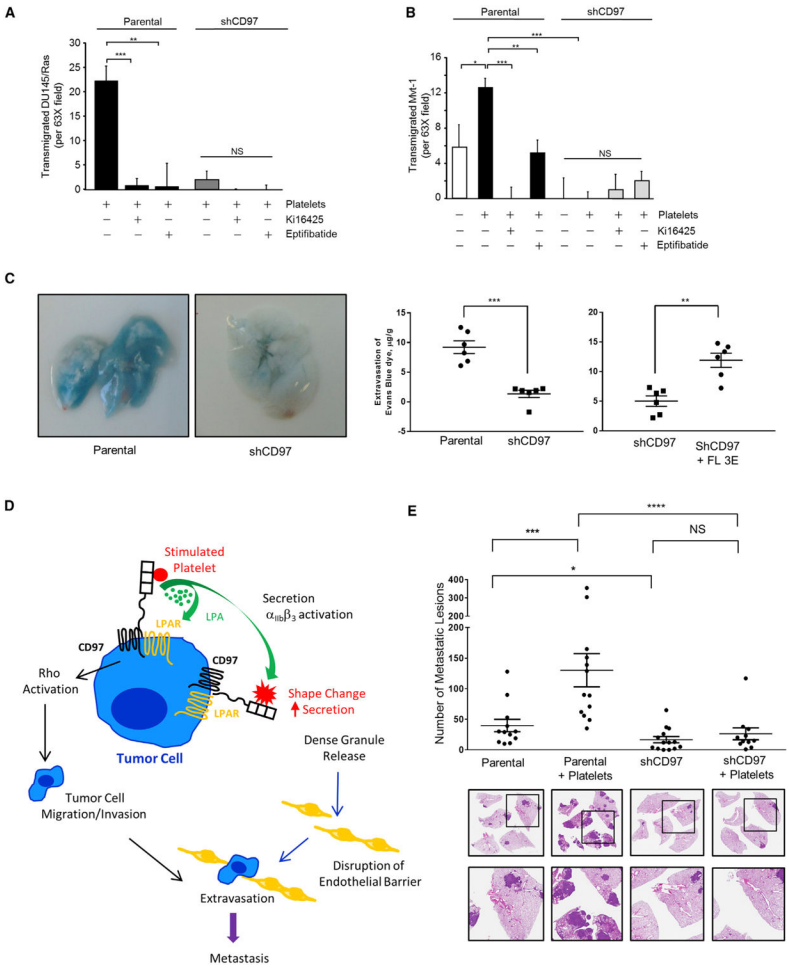

Figure 5. CD97 Is Required for *In Vitro* Platelet-Stimulated TEM, *In Vivo* Tumor-Induced Vascular Permeability, and Experimental Lung Metastasis

(A and B) Effect of (20 μM) Ki16425 or (6 μM) eptifibatide on TEM of DU145/Ras cells (A) or Mvt-1 cells (B) in the absence or presence of platelets. Tumor cells were seeded on a monolayer of endothelial cells (HUVEC) in the top chamber of a Transwell and transmigration to a chemoattractant (5% FCS) was assayed. All results shown are representative of at least 4 independent experiments. Error bars represent ± SEM.

(C) Left: representative Evans blue lung staining in mice injected via the tail vein 24 hr earlier with parental or CD97-depleted (shCD97) Mvt-1 tumor cells. Right: spectrophotometric quantification of Evans blue extracted from the lungs of mice injected 24 hr earlier with parental, CD97-depleted (shCD97), or reconstituted (ShCD97 + FL-3E) Mvt-1 tumor cells (n = 6). Mean values ± SEM for all individuals within a cohort are indicated. All results shown are representative of at least 2 independent experiments.

(D) Schematic depicting a model whereby the interaction of platelets with CD97 initiates rapid bidirectional signaling and coordinates the timing of tumor migration and endothelial junction disruption.

(E) Scatterplot showing numbers of metastatic foci per animal in H&E stained sections of all lung lobes 14 days following tail vein injection of parental or CD97-depleted (shCD97) Mvt-1 cells pretreated with buffer or platelets for 20 hr (n = 12−14). Mean values ± SEM for

all individuals within a cohort are indicated. Representative lung foci in H&E stained sections for each category are shown.

The p values for all panels were calculated by two-tailed unpaired t test. *p < 0.05; **p < 0.01; ***p < 0.001; ****p < 0.0001; NS, not significant.

See also Figure S4.

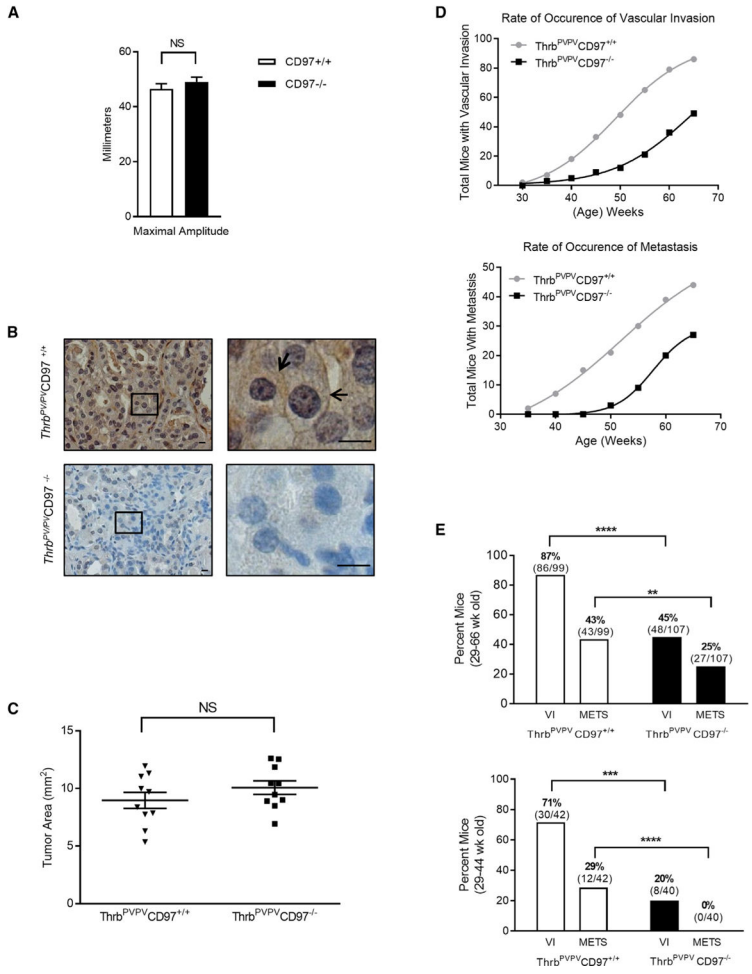

Figure 6. CD97 Is a Determinant Of Metastatic Potential in a Model of Endogenous, Progressive Thyroid Cancer

(A) Whole blood thromboelastogram assay of platelet function in CD97$^{+/+}$ and CD97$^{-/-}$ mice (n = 6) following arachidonic acid initiated platelet aggregation. No significant difference (NS) determined by unpaired t test.

(B) Immunohistochemical staining of mouse CD97 in representative primary thyroid tumors from *Thrb*$^{PV/PV}$ CD97$^{+/+}$ mice expressing wild-type CD97 or *Thrb*$^{PV/PV}$ CD97$^{-/-}$ animals. Arrows indicate membrane staining.

(C) Relative tumor area of primary thyroid tumors in 29- to 44-week-old *Thrb*^{PVPV} CD97$^{+/+}$ compared to *Thrb*^{PVPV} CD97$^{-/-}$ mice. No significant difference (NS) determined by unpaired t test.

(D) Rate of developing vascular invasion (top) or metastasis (bottom) is shown as the cumulative number of mice over time exhibiting tumor cells in blood vessels or metastatic foci in lungs, respectively. The slopes of the two lines in each panel are significantly different (vascular invasion p = 0.00014; metastasis p = 0.018)

(E) Relative incidence of vascular invasion (VI) and metastasis (METS) in *Thrb*$^{PV/PV}$ CD97$^{+/+}$ mice (n = 99) compared with *Thrb*$^{PV/PV}$ CD97$^{-/-}$ mice (n = 107). Top: data for all animals in the study. Bottom: results for younger animals (29–44 weeks) only. **p < 0.01;

***p < 0.001; ****p < 0.0001. The actual number of positive animals is shown in parentheses.

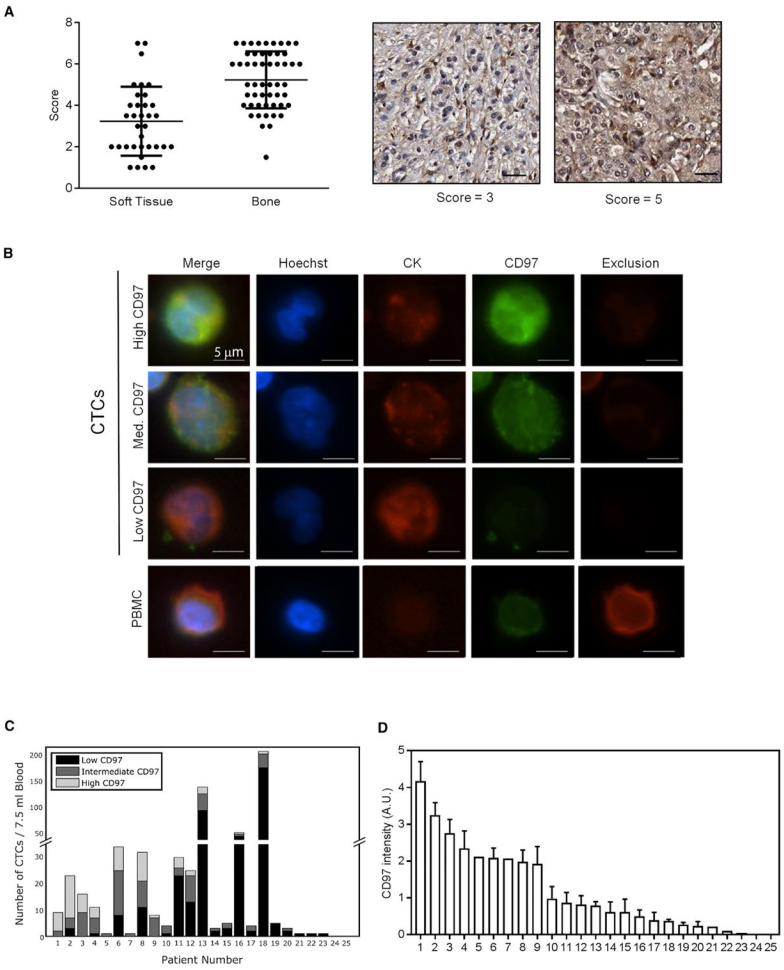

Figure 7. Prostate Cancer Metastases and Circulating Tumor Cells Express CD97

(A) Relative scores for CD97 staining of tissue microarrays composed of prostate soft tissue and bone metastatic lesions. Representative staining for soft tissue cores with scores of 3 and 5 are shown.

(B) CTCs from patients with prostate cancer were isolated, stained, and imaged using the VERSA and capturing with an anti-Epcam antibody. Representative cytokeratin-positive epithelial cells (CK^+) with high, medium, and low levels of CD97 protein are shown. A representative excluded PBMC, positive for hematopoietic markers, is shown for comparison.

(C) The number of CTCs isolated for each patient is shown. The CTCs, categorized as low, intermediate, or high for CD97 staining is shown for each patient.

(D) The mean intensities of CD97 staining for CTCs are shown for each patient.

See also Figure S5.